

EIGHTH EUROPEAN ROTORCRAFT FORUM

APPLICATION OF AN ANALYTIC STALL

MODEL TO DYNAMIC ANALYSIS OF ROTOR BLADES

J. P. ROGERS*

GRADUATE STUDENT
WASHINGTON UNIVERSITY
ST. LOUIS, MISSOURI, USA

August 31 through September 3, 1982

AIX-EN-PROVENCE, FRANCE

ASSOCIATION AERONAUTIQUE ET ASTRONAUTIQUE DE FRANCE

Paper 0.1

*Presently at US Army Aviation Research and Development Command,
St. Louis, Missouri, USA

Application of an Analytic Stall Model
to Dynamic Analysis of Rotor Blades

J. P. Rogers
Washington University
St. Louis, Missouri, USA

ABSTRACT

A dynamic analysis of a rotor blade is performed, including an analytic model for blade stall. The normal lift force on the blade element is determined throughout the linear and non-linear regimes of angle of attack from a simplified version of the stall model of Tran and Petot⁽¹⁾. Blade-element theory is used to investigate the forced and transient response of a single rotor-blade element, hinged in the flapping degree of freedom. The analysis shows that this dynamic stall model may be easily incorporated into conventional, blade-element theory; and this results in a more realistic estimate of blade response than can be predicted by classical linearized theory.

1. NOTATION

- a = linear static lift curve slope, per degree
 a_i = coefficients of the non-linear static lift curve polynomial
 b = blade element semi-chord, equal to $c/2$, m
 c = blade element chord, m
 C = phase shift parameter
 C_L = total lift coefficient
 C_{L1} = lift coefficient in linear regime
 C_{L2} = lift coefficient in non-linear regime
 C_{Ll} = static lift coefficient in linear regime
 C_{Ls} = static lift coefficient, approximate expression
 C_{L0} = actual static lift coefficient
 ΔC_L = difference between the extended linear static lift coefficient (C_{Ll}) and the actual static lift coefficient (C_{L0}).
 d = blade element span, m
 k = reduced frequency $k = \frac{\omega b}{2V}$ (Ref. 1), $k \equiv b/x$ (here).
 k_β = blade flapping restraint spring constant, N-m/rad
 M = Mach number
 P = non-dimensional blade flapping frequency, per revolution
 Δ = apparent mass parameter
 t = time, sec
 $u(\theta)$ = unit step function
 V = average blade element velocity, $V = \Omega x$, ft/sec
 x = distance from center of rotation, m
 α = damping parameter
 β = blade flapping angle, deg.
 γ = Lock number
 $\bar{\gamma}$ = natural frequency parameter

1. NOTATION (CONT.)

δ	=	parameter relating lift and airfoil pitch rate
Θ	=	total aerodynamic angle of attack, deg
$\Theta_o, \Theta_s, \Theta_c$	=	mean angle of attack (collective pitch) and cyclic pitch, deg.
Θ_{cr}	=	airfoil critical angle of attack, deg.
$\hat{\Theta}$	=	amplitude of airfoil oscillation, deg.
λ	=	time delay parameter
μ	=	advance ratio
τ	=	reduced time, $\tau = \Omega r t / b$
ψ	=	azimuth angle, $\psi = \Omega t = k \tau$
Ω	=	rotor speed, rad/sec
ω	=	airfoil frequency of oscillation, rad/sec
$(\cdot), (\cdot\cdot)$	=	$\partial/\partial \tau, \partial^2/\partial \tau^2$ (derivatives with respect to reduced time,)

2. INTRODUCTION

Conventional rotor dynamic analysis does not include the effects of blade stall at high angles of attack. Instead, conventional analysis is based on a linearized aerodynamic model which assumes a constant lift-curve slope throughout the operating range of angle of attack. Thus, such analyses cannot produce an accurate representation of the blade response at high lift or high speed. There are, however, more advanced analysis tools that attempt to include the non-linearities associated with stall⁽²⁻⁴⁾. These analyses are generally cumbersome and rather inconvenient to use in research or preliminary design applications. Existing stall models usually involve the tabularization of large quantities of measured, wind-tunnel data. A table look-up and interpolation scheme is then used to gather data for each particular angle of attack that occurs during the analysis. The major underlying drawbacks of these methods are: 1) theoretical analysis is limited to only those test conditions that were measured experimentally, thus making extrapolation to other conditions very difficult, 2) the tabular nature of the model makes it inconvenient (if not impossible) to obtain linearized equations for stability analysis, and 3) the constant necessity of computer search slows the computation, thus making it more expensive. Bielawa (Reference 5) and Gangwani (Reference 6) have used advanced mathematical techniques to develop stall models that do not use the table look-up scheme previously mentioned. However, the resulting set of analytic expressions are again difficult to linearize for use in stability analysis. Therefore, the need exists for a simple, analytical method that can model the stall of an oscillating airfoil, that can be easily incorporated into blade dynamic theory, and that will produce accurate results over a wide range of aerodynamic parameters.

Tran and Petot⁽¹⁾ of ONERA have made a quantum leap in the development of such an analytical stall model. The stall model is semi-empirically derived using measured wind tunnel data for an oscillating airfoil in conjunction with a parameter identification scheme. The result is a set of differential equations that relate the normal lift coefficient

of an airfoil to angle of attack and its time derivatives.* Although Tran and Petot identify their model on the basis of small oscillations ($\pm 1^\circ$), they correlate results for $\pm 6^\circ$ oscillations about a full range of mean values of angle of attack. Comparisons of the analytical stall model to measured wind-tunnel data at these conditions show excellent correlation.

The purpose of this paper is three-fold: 1) to verify the results of the Tran and Petot stall model analysis and then investigate possible modifications of the equations that would make them more compatible with standard rotor-blade dynamic analysis, 2) to apply the modified stall model to the forced response of a simple rotor-blade element, and 3) to study the transient response and stability of the rotor blade element in hover and forward flight. A single blade element is employed for simplicity, but the analysis and conclusions are easily extended to an entire blade. The response of the single, flapping, blade element is calculated (including the simplified analytic stall model) by numerical integration, Floquet theory, and classical eigenvalue analysis. The results are compared to classical linearized theory.

3. STALL MODEL

The analytical stall model presented here is that of Reference 1. The model consists of three equations that relate the lift coefficient of an airfoil to its angle of attack as follows

$$\dot{C}_{z_1}^* + \lambda C_{z_1} = \lambda C_{z_1} + (\lambda \Delta + \delta) \dot{\Theta} + \Delta \dot{\Theta}^* \quad (1)$$

$$\dot{C}_{z_2}^* + 2\alpha \bar{\gamma} \dot{C}_{z_2}^* + \bar{\gamma}^2 (1 + \alpha^2) C_{z_2} = -\bar{\gamma}^2 (1 + \alpha^2) \left[\Delta C_z + \bar{c} \frac{\partial \Delta C_z}{\partial \Theta} \dot{\Theta} \right] \quad (2)$$

$$C_z = C_{z_1} + C_{z_2} \quad (3)$$

where (*) represents a derivative with respect to reduced time; and where C_{z_1} and C_{z_2} are the normal lift coefficients in the linear and non-linear regions of angle of attack, Θ is the total aerodynamic angle of attack of the airfoil in degrees, C_{z_1} is the static lift coefficient in the linear region of angle of attack, ΔC_z is the difference between the extended linear lift curve ($C_{z_1} = \alpha \Theta$) and the actual static lift curve (C_{z_0}), and C_z is the resulting total lift coefficient. The parameters are functions of blade angle of attack alone (for a given airfoil) and must be determined from wind tunnel tests by parameter identification. Tran and Petot performed such tests and identified the parameters for an ONERA, OA212 airfoil. The tests were performed at small amplitudes

*Ref. 1 also treat pitching moment data, but pitching moment is not included in the analysis of this present paper.

of oscillation (less than 1°) about incremental angles of attack at various reduced frequencies. This method of testing served to effectively linearize the equations about each mean angle of attack. Values of the parameters were then determined in the linear and non-linear regions of mean angle of attack. The parameters from those tests are independent of reduced frequency. This is important to the application of the theory because in rotor problems no single reduced frequency can be defined. The parameters are given by

$$\lambda = 0.20 \quad (4)$$

$$\Delta = 5\pi/180 \quad (5)$$

$$\delta = \partial C_{z2} / \partial \theta - 4\pi [1 + 1.43 \Delta C_z] / 180 \quad (6)$$

$$\bar{\gamma} = 0.10 + 0.023 (\theta - 13^\circ) u(\theta - 13^\circ) \quad (7)$$

$$\alpha = 0.105 / \bar{\gamma} \quad (8)$$

$$\bar{c} = 2 - 5.1 \tan^{-1} \{ 1.21 (\theta - 13^\circ) \} u(\theta - 13^\circ) \quad (9)$$

where λ is a time delay parameter, Δ is the apparent mass quantity, δ is a parameter that relates the lift coefficient to the pitch rate of the airfoil, $\bar{\gamma}$ is the natural frequency, α is a damping factor, and \bar{c} is a phase-shift parameter. The term $u(\theta - 13^\circ)$ is a unit step function; $u(\theta - 13^\circ)$ is zero for angle of attack less than 13° and is 1 for angles of attack greater than or equal to 13° .

The static lift curve of the OA212 airfoil is presented in Figure 1. The curve is defined in the linear region by the equation

$$C_{zS} = \frac{7.1\pi}{180} \theta \quad \text{for } \theta \leq \theta_{cr} \quad (10)$$

and in the non-linear region by the seventh order polynomial

$$C_{zS} = \sum_{i=0}^7 a_i (\theta - 10^\circ)^i \quad \text{for } \theta \geq \theta_{cr} \quad (11)$$

where the a_i are

$$\begin{aligned} a_0 &= 1.24 \\ a_1 &= 0.124 \\ a_2 &= 0.0630597 \\ a_3 &= 0.01395201 \\ a_4 &= 0.0017390851 \\ a_5 &= 0.00012451913 \\ a_6 &= 4.6849257 \times 10^{-6} \\ a_7 &= 7.087973 \times 10^{-8} \end{aligned} \quad (12)$$

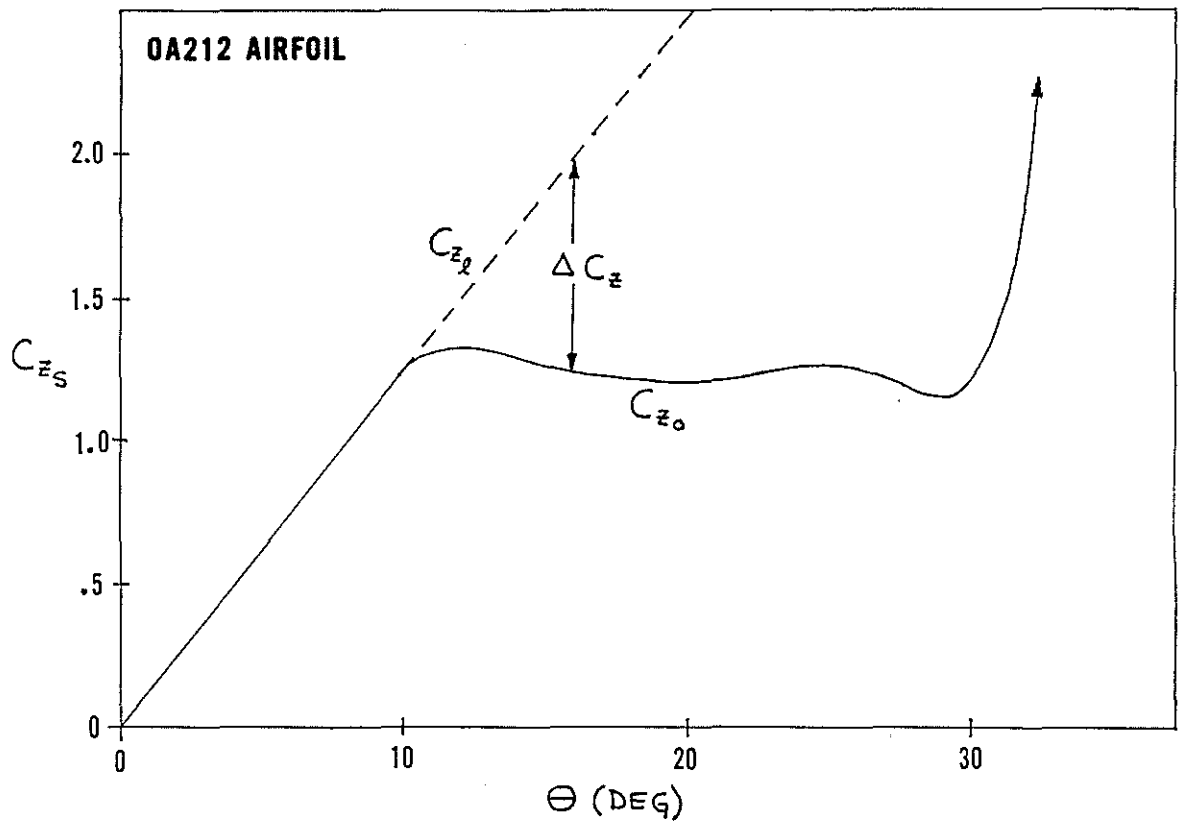


FIGURE 1
STATIC LIFT COEFFICIENT VERSUS ANGLE OF ATTACK

In order to validate their identified stall model, Tran and Petot have performed tests at large amplitudes of oscillation (up to $\pm 6^\circ$) for various mean values of angle of attack. The results of these analyses are compared to the experimentally measured values in Ref. (1). Figure 2 is a reproduction of the plots of normal lift coefficient C_z versus the angle of attack (from Ref. 1) for various values of the mean angle of attack. All results are for oscillations of $\pm 6^\circ$ at a reduced frequency of .05 (based on $k = \omega b / \alpha x$). Experimental data are presented for the aforementioned OA212 airfoil, which has a static stall angle of attack, $\Theta_{cr} = 10^\circ$. Good correlation between theory and experiment can be seen throughout the range of angle of attack 0° to 16° .

4. STALL MODEL VERIFICATION

The first step in the present application of the stall model to rotor dynamic analysis is to verify the validity of the model by reproduction of the previously published lift hysteresis loops. Thus, the stall model, equations 1-3, is transformed into a computer code that uses a Runge-Kutta method of numerical integration for solution. Figure 3 shows the results of this analysis in the form of C_z versus Θ . The mean angle of attack, oscillatory angle of attack, and blade parameters are the same as in Figure 2 in order to facilitate the comparison. The hysteresis loops tend to take on an ellipsoidal appearance when angle-of-attack excursions do not exceed the static stall angle of attack. As slightly higher mean angles of attack are encountered, the loops tend to take on figure eight shapes; and at mean angles of attack well above stall, the loops are more erratic. The results of these initial computations generally duplicate the published data of Reference 1 for mean angles of attack of 11° or less. For mean angles of attack between 12° and 14° , however, oscillations appear in the lower portion of the lift curve; and these are not found in the published data of Reference 1. Upon closer scrutiny, one finds that the oscillations do indeed occur from the solution of equations (1) - (3). However, when a relatively coarse step size is used in the integration, the oscillations are effectively filtered out of the response. We assume that such an unconscious filtering occurs in Ref. 1. Thus, the curves that are presented in this section are probably a more accurate representation of the behavior of the stall model than are those of Reference 1. This would indicate that further refinement of the model may be in order, and this could be a topic of further research.

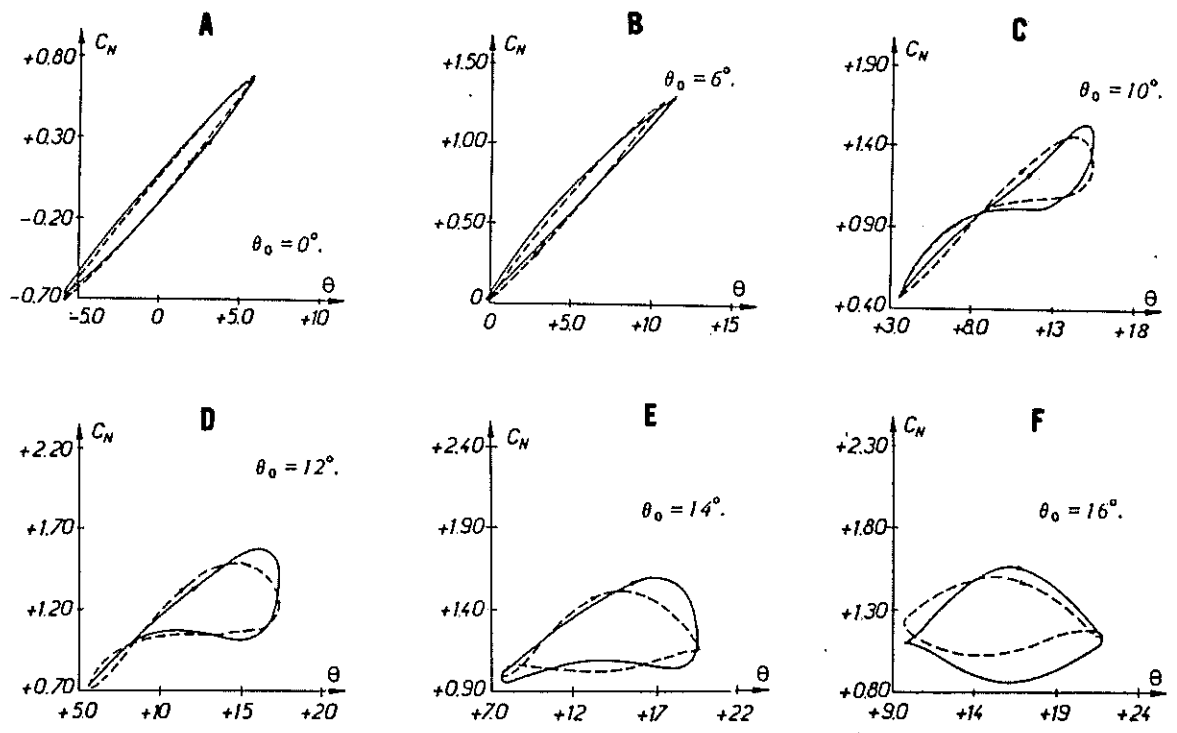


FIGURE 2
LIFT COEFFICIENT VERSUS ANGLE OF ATTACK
(REFERENCE 1) $M=0.30, k=0.05, \tilde{\Theta} = 6^\circ$

OA212 AIRFOIL

———— EXPERIMENT
 - - - - MODEL
 > SENSE OF GYRATION

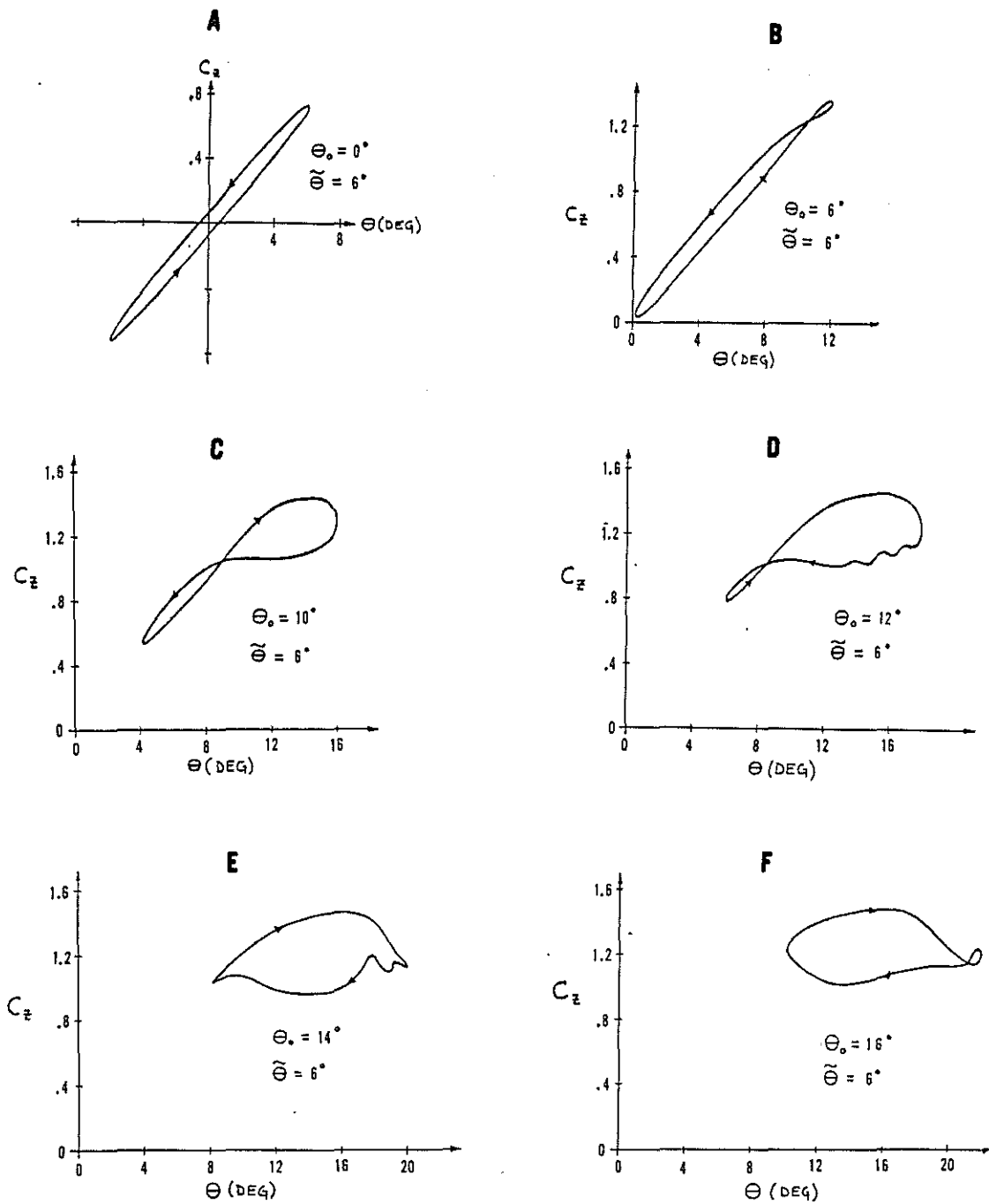


FIGURE 3
LIFT COEFFICIENT VERSUS ANGLE OF ATTACK
OA212 AIRFOIL
M=0.30 k=0.05

Generally, however, the model of Ref. 1 gives an accurate representation of measured experimental data and seems valid for use in dynamic analysis. Furthermore, there is some possibility that the oscillations in the C_z curve may reflect the true unsteady condition on the airfoil. Such unsteadiness is usually averaged out of data and thus would not show up in experimental results even if it existed. Another anomaly discovered by our work is the representation of C_{z_0} by C_{z_5} . The polynomial used for C_{z_5} , equation (11), is found to diverge in an unrealistic manner for $\Theta > 26^\circ$, as seen in Figure 1. Therefore, in the present analysis, a constant value of static lift coefficient ($C_{z_5} = .126$) is used for $\Theta > 26^\circ$. Such angles can, of course, occur at high advance ratios or inboard on the blade.

5. SIMPLIFICATION OF STALL MODEL

The next step in the research reported here, is to study the stall model for possible simplifications. A natural candidate for simplification is the elimination of some of the time derivative terms involving $\dot{\Theta}$ and $\ddot{\Theta}$ (apparent mass and angular rate terms). These terms are good candidates for elimination on at least two counts. First, they are almost always eliminated in classical rotor-blade analyses; and, second, their retention (especially $\ddot{\Theta}$) results in a cumbersome complication in the state variable equations for rotor flapping. Therefore, it is useful to study the effects of $\dot{\Theta}$ and $\ddot{\Theta}$ terms on the stall model. In the first study, the lift hysteresis loops are generated with $\Delta, \bar{C}, \bar{S} = 0$ in equations (1) and (2) (no $\dot{\Theta}$ or $\ddot{\Theta}$ term). Figure 4 shows C_z versus Θ for $\bar{\Theta} = 6^\circ$ and at two typical mean angles of attack. The resulting plots are not all similar to the original results presented in Figure 3. Therefore, the stall model is oversimplified by elimination of all three parameters. Further investigation, however, shows that setting only the parameter Δ to 0 produces a negligible effect on the hysteresis loops. An example is given in Figure 5 which gives C_z versus Θ with the parameter $\Delta = 0$. These plots show the negligible effect of Δ on the lift curves. One may reasonably conclude that Δ may be deleted from the stall model. One might argue that only the $\dot{\Theta}$ term should be removed from equation (1) with $\Delta \lambda$ remaining on the $\dot{\Theta}$ term. As it turns out, however, $\Delta \lambda$ is only 12% of the total $\dot{\Theta}$ term ($\Delta \lambda + \bar{S}$) so that either approximation would be valid. Further studies of the model with \bar{S} or \bar{C} removed separately show that both are important parameters. This is very interesting since the $\dot{\Theta}$ term has been used very little in linearized rotor analyses.

6. ROTOR BLADE MODEL

The rotor blade model used in the dynamics application of the simplified stall model is presented in Figure 6. The model consists of a single blade element located at a radial position x from the center of rotation. A single blade element is used here for simplicity, since the entire analysis may be easily extended to include a complete blade. Two forces act on the blade element: 1) the centrifugal force,

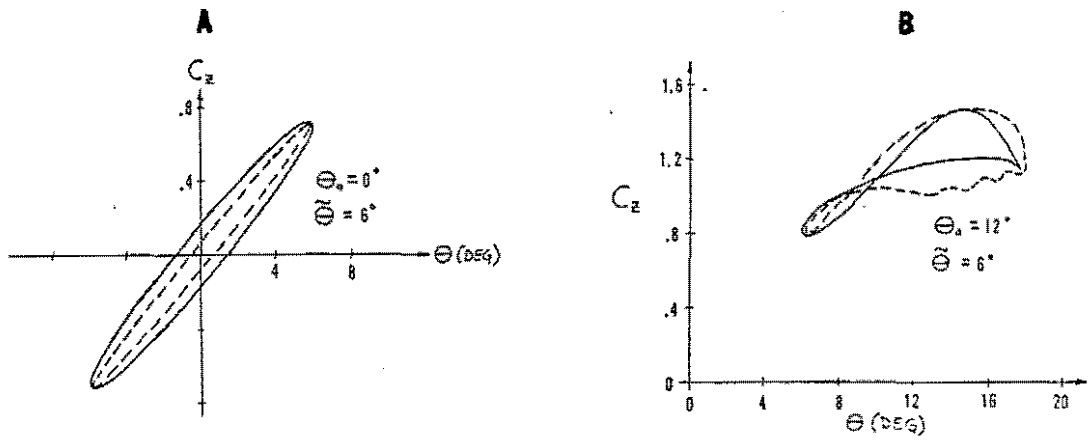


FIGURE 4
LIFT COEFFICIENT VERSUS ANGLE OF ATTACK
 ——— $\Delta, \bar{c}, \delta = 0.0$
 - - - - - BASELINE

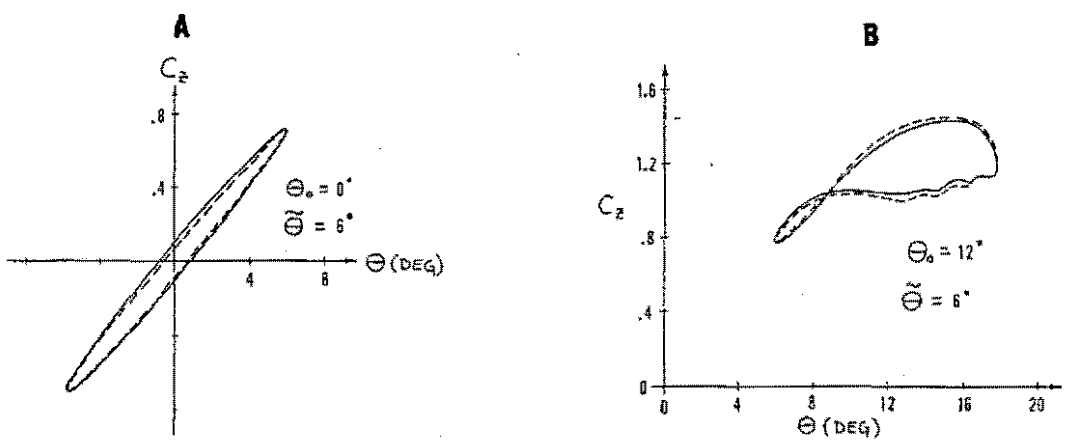


FIGURE 5
LIFT COEFFICIENT VERSUS ANGLE OF ATTACK
 ——— $\Delta = 0.0$
 - - - - - BASELINE

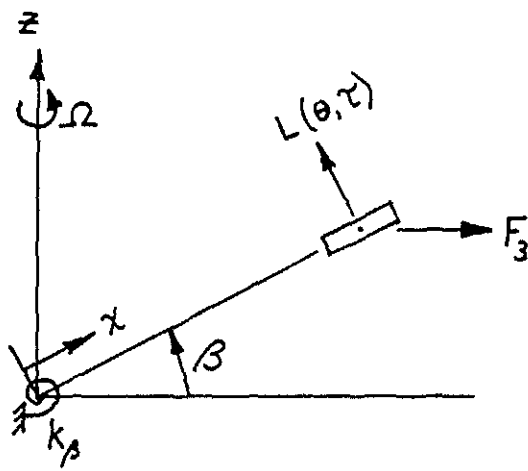


FIGURE 6
ROTOR BLADE MODEL

F_z , and 2) a normal lift force, L , which is a function of angle of attack, θ , and reduced time, τ . The blade is allowed to flap with angle, β , and is restrained in the flapping direction by a root spring, $k\beta$. The angular velocity of the blade element about the hub is Ω . Physical dimensions of the element are c (the chord), d (the span), and b (the semi-chord).

From blade-element theory, the flapping equation of motion may be written in non-dimensional form as

$$\beta^{**} + k^2 p^2 \beta = \frac{\gamma}{8} \frac{k^2}{a} C_z(\theta, \tau) (1 + 2\mu \sin k\tau + \mu^2 \sin^2 k\tau) \quad (13)$$

where β is the flapping angle in degrees, k is defined as the reduced frequency based on rotor speed ($k = b/x$), p is the non-dimensional flapping frequency, γ is the Lock number, C_z is the normal lift coefficient which is a function of angle of attack θ and reduced time τ , a is the linear static lift curve slope, and μ is the advance ratio. Degrees are used as units for β so that β can be more easily incorporated into the angle of attack terms to follow. The units of a on the right-hand side of equation (13) are per/degree so that everything is consistent. The $(^*)$, $(^{**})$ operators represent derivatives with respect to reduced time τ . The reduced time is related to the azimuthal angle of the blade by a non-dimensional reduced-frequency based on rotor speed, k .

$$\tau \equiv \Omega x t / b \quad (14)$$

$$k \equiv b/x \quad (15)$$

$$\psi = k\tau = \Omega t \quad (16)$$

It is emphasized that no assumption has been made concerning the frequency of oscillation. The definition $k = b/x$ follows directly from the change of variable in equation (14). The simplified stall model enters the flapping equation of motion through the quantity $C_z(\theta, \tau)$, which serves to couple the dynamics and aerodynamics.

The true aerodynamic angle of attack of the blade element, θ , is given by

$$\theta = \theta_0 + \theta_s \sin k\tau + \theta_c \cos k\tau - \left[\frac{\beta/k + \mu \beta \cos k\tau}{1 + \mu \sin k\tau} \right] \quad (17)$$

where θ_0 is the mean angle of attack (collective pitch minus inflow angle) and θ_s and θ_c are the cyclic pitch (also including inflow variations). For linearized theory, the rotor disk is trimmed by

$$\theta_s = -2\mu \theta_0 \quad (18)$$

$$\theta_c = \frac{\gamma \mu}{8 p^2} \theta_0 \quad (19)$$

For quasi-steady theory, $k = 0$. The quasi-steady values of Θ_s and Θ_c are used here. The bracketed term in equation (17) represents the angle of attack induced by the blade flapping motion. The first derivative of Θ with respect to τ appears in the stall model and is given by

$$\dot{\Theta} = \Theta_s k \cos k\tau - \Theta_c k \sin k\tau - \left[\frac{\beta^*/k + \mu \beta^* \cos k\tau - \mu \beta k \sin k\tau}{1 + \mu \sin k\tau} \right] + \left[\frac{\mu \beta^* \cos k\tau + \mu^2 \beta k \cos^2 k\tau}{(1 + \mu \sin k\tau)^2} \right] \quad (20)$$

There are five aspects of equations (17) and (20) that need comment. First, the Tran and Petot model does not distinguish between angle of attack due to blade pitch and angle of attack due to vertical velocity components. It could be argued that (except for apparent mass effects) these should be similar. On the other hand, one cannot be sure of this until further tests are done. Second, the Tran and Petot model is for a fixed airfoil and not for a rotating blade. It may very well be that the parameters will be significantly different and strongly lift-dependent for a rotating airfoil. Third, we note that for a rotor, there is a "steady" pitch rate term, $\dot{\Theta} = k\beta$, due to the component of Ω along the blade. However, this term has not been used in previous rotor analyses and we neglect it here, also. Fourth, the Tran and Petot model does not account for unsteadiness in the free stream, although such unsteadiness is present in rotors. Future work on the effect of unsteady velocity needs to be done. Fifth, equations (17) and (20) show that Θ is dependent on β and β^* . Since the coefficients δ , $\bar{\delta}$, \bar{c} (eqn: 1 and 2) are functions of Θ , a non-linearity is implied in the combined system of equations. This non-linearity is important to the forced response; and it can create periodic coefficients in the linearized equations, as will be shown later.

7. FORCED RESPONSE

The combined set of simplified-stall-model and blade-dynamic equations form a fifth-order system. State variables are introduced into this system and the resulting equations are solved by use of a predictor-corrector numerical integration routine. The integration is carried out over a number of cycles to ensure that all transients have decayed. The forced response of the combined stall-model/blade-dynamics system is presented initially for the following parameters.

$$M = 0.30, k = 0.05, \delta = 6.0, p = 1.0, \mu = 0.20$$

The choice, $k = .05$ implies $b/x = .05$. Later on, variations will be made in μ and k . A mean angle of attack of 10° is chosen so that the airfoil will oscillate well into the linear and non-linear portions of the lift curve. Thus, the effect of dynamic stall on the response of the airfoil can be seen.

Figure 7 presents the results obtained from the combined stall-model, blade dynamic system for the above baseline parameters. Figure 7a shows the typical figure-eight form of C_z versus Θ . The results of conventional linearized analysis are also presented in Figure 7a for comparative purposes. Use of these initial parameters yields a cyclic variation in angle of attack of approximately $\pm 6^\circ$ from the mean value. Figure 7b is a plot of the flapping angle β versus the azimuthal angle ψ . The average β with the model that includes dynamic stall is less than that predicted by linear theory. This can be attributed to the over-prediction of lift on the airfoil by the linearized model at high angle of attack. The 90° phase lag between lift force and blade response is evident from Figure 7b. At $\psi = 270^\circ$ the blade element is stalled; and 90° later ($\psi = 360^\circ$), the flapping angle is reduced to a minimum. Figure 7c shows the cyclic variation of Θ versus ψ . Here, the blade element is above the static stall angle of attack (10°) for $\psi = 180^\circ$ to $\psi = 360^\circ$, which corresponds to the retreating side of the rotor disk. Differences in angle of attack between stall-model analysis and linear theory arise from the different flapping angles predicted by the two theories. (Recall that the flapping angle is included in the angle of attack, equation (17).) Comparison of Figures 7b and 7c shows that, as the flapping angle decreases, the angle of attack correspondingly increases, which forces the blade deeper into stall.

Similar analyses have been performed over a range of advance ratio μ and reduced frequency k and are presented in Reference 8. In the linear portions of the lift curves, the linear theory and stall model show fairly good correlation. Figure 8 is for $\mu = 0.30$, $k = 0.05$, $\gamma = 6.0$, $p = 1.0$, $M = 0.30$. At this rather high value of advance ratio, an erratic behavior is seen in the C_z versus Θ curve (Figure 8a). This behavior is due to the stall model and stems from the high angles of attack that are encountered at this advance ratio. However, the flapping response remains relatively unaffected as can be seen in Figure 8b. This anomaly was mentioned earlier in this paper and should be the subject of further research and investigation. For advance ratios less than 0.30 the curves are well behaved.

8. HOVER LIMIT CYCLES

Several cases were studied in Reference 8 to determine the decay of the system response in hover conditions (i.e. $\mu = 0$). Figure 9a shows the flapping angle β plotted against non-dimensional time ψ for a mean angle of attack $\Theta_0 = 10^\circ$ and other parameters $k = 0.05$, $\mu = 0.0$, $p = 1.0$, $\gamma = 6$. Here, β is seen to decay fairly rapidly to a steady-state value of approximately 0.13 radians which indicates that ample damping is available. Figures 9b and 9c again show β versus ψ for angles of attack of 12° and 14° . Figures 9b and 9c show that β does not decay to a steady value but exhibits a limit cycle behavior. This could be due to a very low damping in the system or to an instability in the coupled blade-stall model equations. The same limit cycle behavior is also evident (from Reference 8) for the lift coefficients C_{z1} and C_{z2} , again indicating an instability in the coupled blade-stall system for this angle of attack. This phenomenon will be investigated

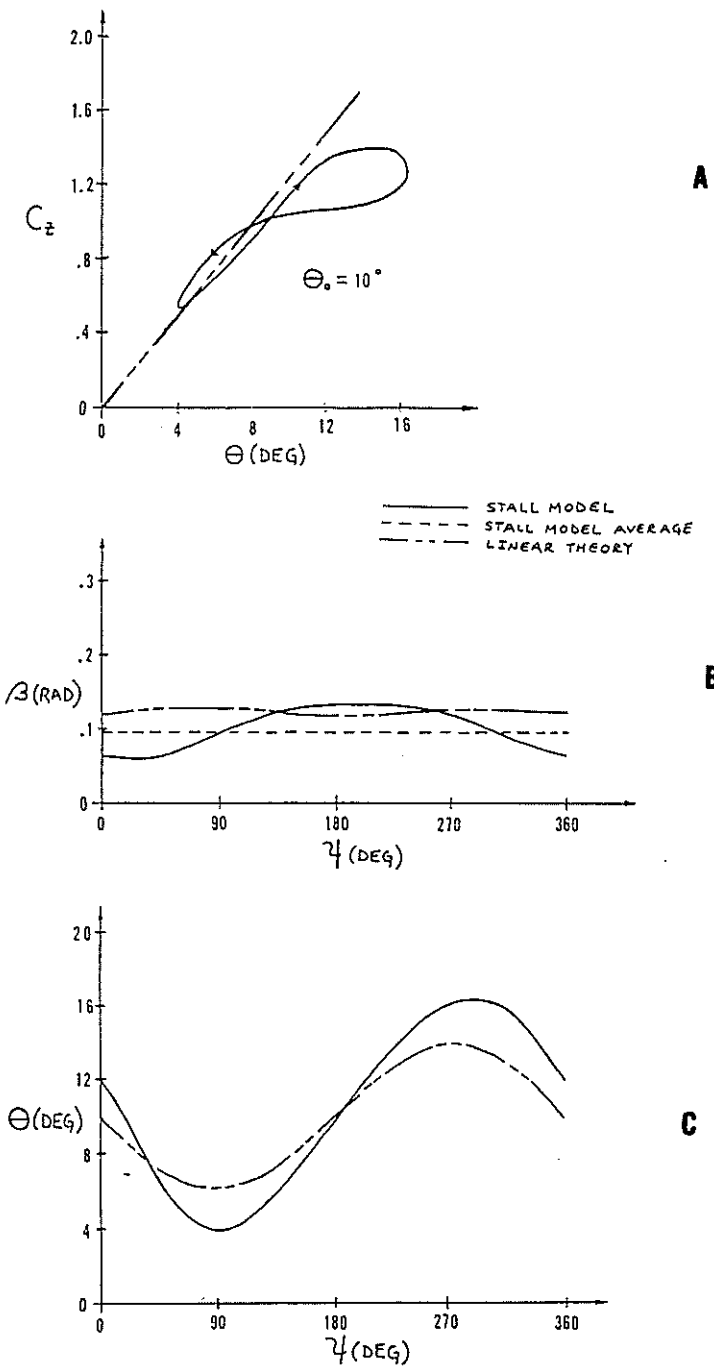


FIGURE 7 FORCED RESPONSE
(A) LIFT COEFFICIENT VERSUS ANGLE OF ATTACK
(B) FLAPPING ANGLE VERSUS AZIMUTH ANGLE
(C) ANGLE OF ATTACK VERSUS AZIMUTH ANGLE
 $k = 0.05$, $\gamma = 6$, $\rho = 1$, $\mu = 0.2$

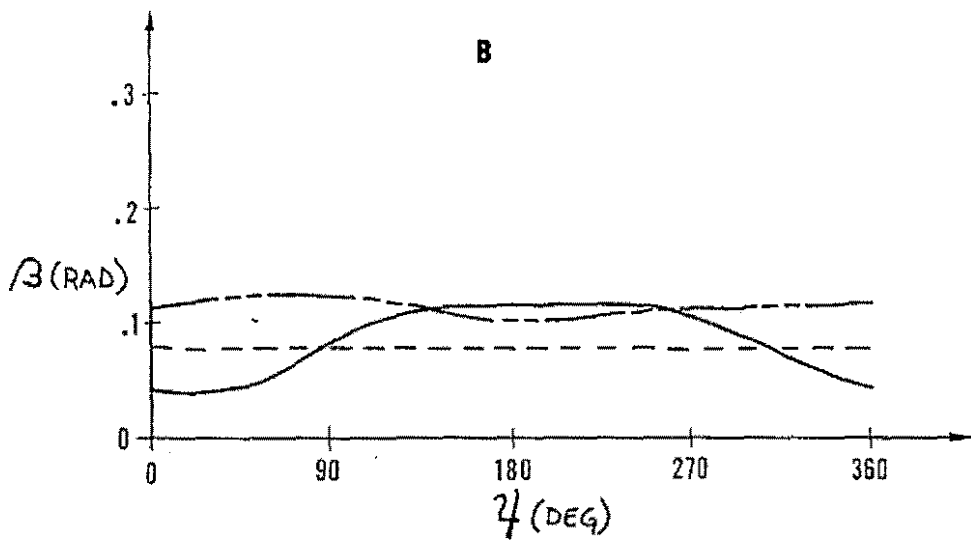
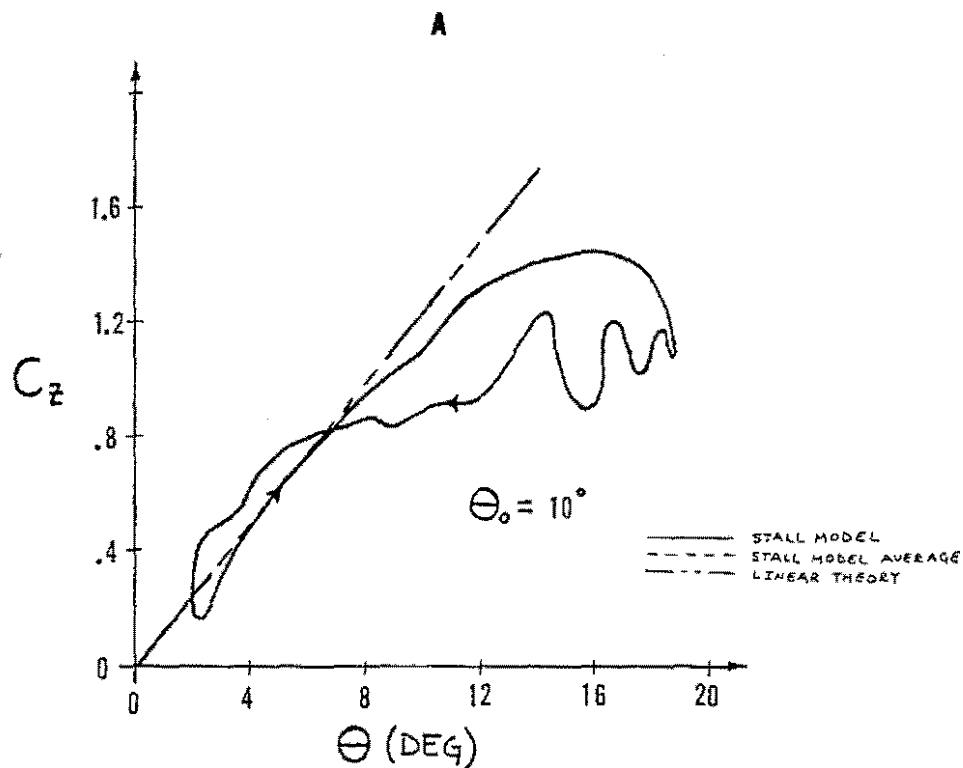


FIGURE 8 FORCED RESPONSE
(A) LIFT COEFFICIENT VERSUS ANGLE OF ATTACK
(B) FLAPPING ANGLE VERSUS AZIMUTH ANGLE
 $k = 0.05, \gamma = 6, p = 1, \mu = 0.3$

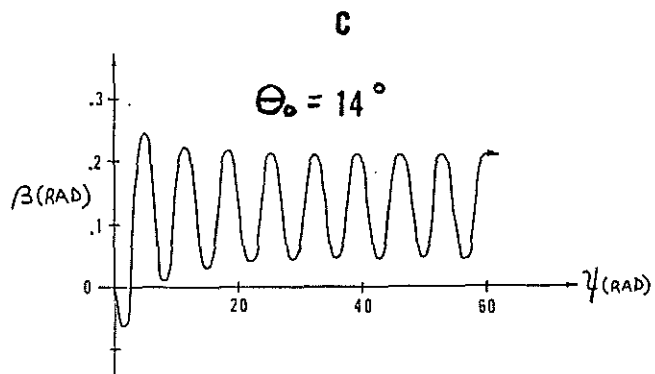
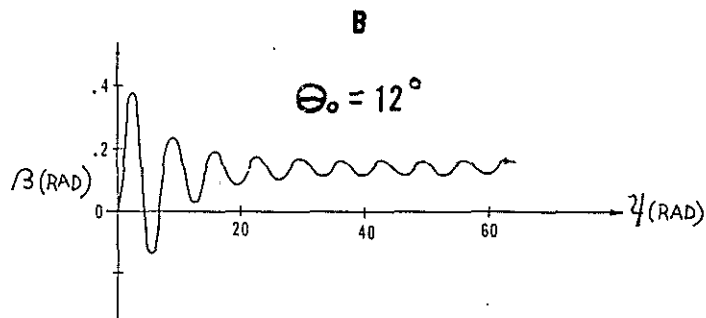
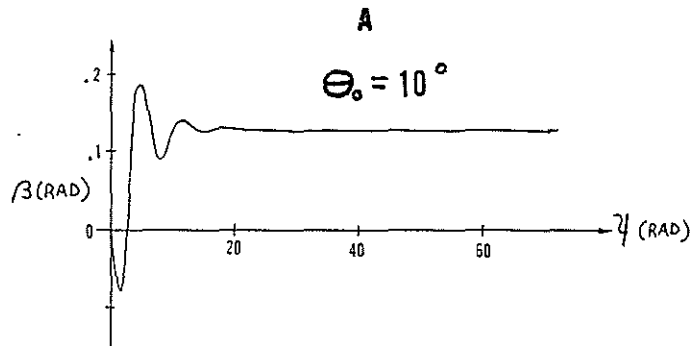


FIGURE 9 HOVER TRANSIENTS
 $k = 0.05, \gamma = 6, p = 1, \mu = 0$

further in the transient-response portion of this paper below.

9. TRANSIENT HOVER RESPONSE

To solve the combined stall model and blade-dynamic equations for the transient response, one must first linearize these equations of motion about a constant (or periodic) equilibrium position to obtain linear, constant-(or periodic) coefficient equations for blade damping and frequency. The introduction of the following perturbation expansions of each variable leads to a set of homogenous equations which can be solved using standard eigenvalue analysis for the case of hover, or by Floquet theory for forward flight.

$$\begin{aligned} \text{Let: } \beta &= \bar{\beta} + \delta(\beta) \\ c_{z_1} &= \bar{c}_{z_1} + \delta(c_{z_1}) \\ c_{z_2} &= \bar{c}_{z_2} + \delta(c_{z_2}) \\ \Theta &= \bar{\Theta} + \delta(\Theta) \\ &\epsilon + c. \end{aligned} \tag{21}$$

where the barred quantities ($\bar{\beta}$, \bar{c}_{z_1} , etc.) are equilibrium values of the variables and the quantities $\delta(\)$ represent small perturbations. Substitution of equations (21) into the combined stall model/blade dynamic system equations results in a set of equations that contain only perturbation quantities and constants.

For the case of hover ($\mu = 0$) the system of perturbation equations reduce to a set of constant coefficient equations. This is due to the constant equilibrium values of angle of attack and flapping angle that occur during the hover condition. Solutions to these equations are found using a standard eigenvalue analysis on a computer. Eigenvalues are extracted and studied for stability. The real part of these complex eigenvalues corresponds to the damping, while the imaginary part represents the frequency (when the roots are plotted in the complex plane). Figure 10 is the root locus plot of frequency versus damping for the β eigenvalue, as a function of mean angle of attack. For a mean angle of attack of 10° , the root is stable. As the mean angle of attack increases, a sudden reduction in frequency and damping occurs and the root finally becomes unstable at approximately 13.2° . From that point the frequency increases slightly and then decreases to zero, at which point two real roots are formed. This stability plot is consistent with the transient response found from numerical integration in Figure 9. For example, at $\Theta = 10^\circ$ the eigenvalue in Figure 10 is $0.019 + 0.047i$ which, in terms of a τ time scale, is $0.38 + 0.93i$ (the same as linear theory). This agrees with the β decay shown in Figure 9a. At $\Theta = 12^\circ$, on the other hand, the eigenvalue analysis shows a nearly neutrally stable root; and Figure 9b shows a weak limit cycle ($+1.5^\circ$). Finally, at $\Theta = 14^\circ$, Figure 10 shows a highly unstable eigenvalue; and Figure 9c shows a strong limit cycle ($+5^\circ$). Thus, the perturbation analysis (although not capable of predicting quantitative values of a limit cycle) nevertheless gives a physically meaningful insight into the rotor-stall behavior.

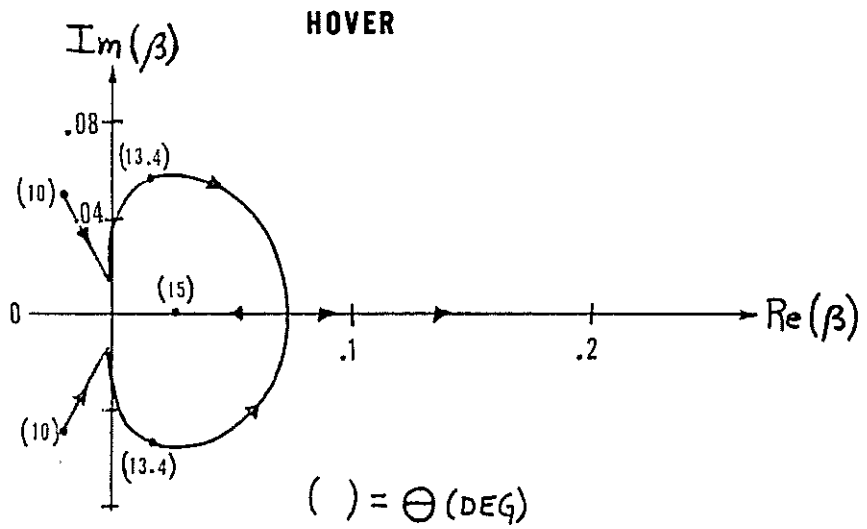


FIGURE 10
FLAP EIGENVALUE ROOT LOCUS
 $k = 0.05, \gamma = 6, \rho = 1, \mu = 0$

10. TRANSIENT FORWARD-FLIGHT RESPONSE

For forward flight (i.e. $\mu \neq 0$), the perturbation equations of motion contain periodic coefficients. The stability of this system of linear differential equations is then determined by Floquet theory. Due to the relative disparity between typical flap damping ($e^{-0.02T}$) and typical stall damping ($e^{-0.16T}$), there is a numerical difficulty in extracting the stall eigenvalues ($e^{-0.16T} \sim 10^{-8}$). In some conditions, there is also a problem of extracting flap eigenvalues. In the results to follow, any eigenvalue of suspicious origin is noted by a solid symbol on the figures.

The equilibrium quantities $\bar{\beta}$ and \bar{C}_{z2} appear as part of the periodic coefficients, and they must be determined from the forced response of the system and then passed to the transient-response analysis. Therefore, tabulated values from the forced-response analysis are used to represent $\bar{\beta}$, \bar{C}_{z2} , and their derivatives by Fourier series. Thus, $\bar{\beta}$ and \bar{C}_{z2} are passed to the transient analysis by means of Fourier coefficients, including the first three harmonics.

Figure 11 is a plot of damping versus advance ratio for a mean angle of attack of 5° . The damping characteristics for each mode (β , C_{z1} , and C_{z2}) are presented in this plot as functions of advance ratio. At a mean angle of attack of 5° (Figure 11) stall is never encountered in the advance ratio range plotted, and all three of the eigenvalues are well behaved. The damping remains at a constant value of -0.022 up to $\mu = 0.79$, at which point the frequency (imaginary part) of this root becomes once per rev (0.05) and two entirely real roots are formed (thus, there are two damping values shown above $\mu = 0.79$). The splitting of eigenvalues at integer-multiple frequencies is a common characteristic of periodic systems and is analogous to the splitting at zero frequency in the constant-coefficient case. In our case, the split is at a higher advance ratio and is more sudden than normally found. This is due to the use of only a single blade element and is also due to the fact that we are trimming out some of the periodic effects with θ_s and θ_c . The C_{z2} damping remains at a constant value of -0.105 throughout the range of advance ratio 0.0 to 1.0. This is to be expected as the angle of attack never exceeds the critical value and thus the system is dominated by the linear (C_{z1}) lift equation with the non-linear (C_{z2}) lift equation effectively eliminated. Some slight unsteadiness is shown for the C_{z1} damping curve for an advance ratio less than 0.40. This was unexpected and is probably due to round-off error in the numerical integration used in the analysis. This unsteadiness does settle out for advance ratios above 0.40, and the damping remains at a constant value of -0.155.

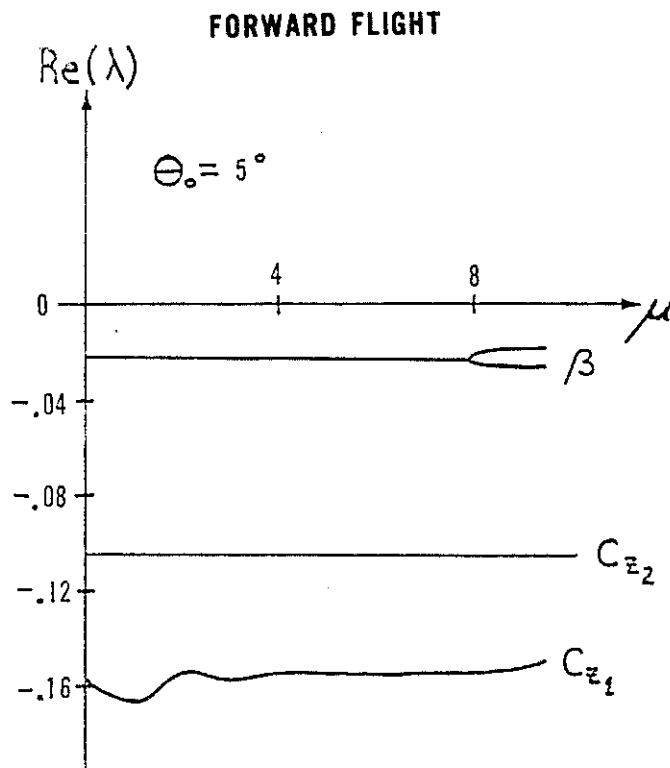


FIGURE 11
DAMPING VERSUS ADVANCE RATIO

$k = 0.05, \gamma = 6, p = 1$

FOWARD FLIGHT

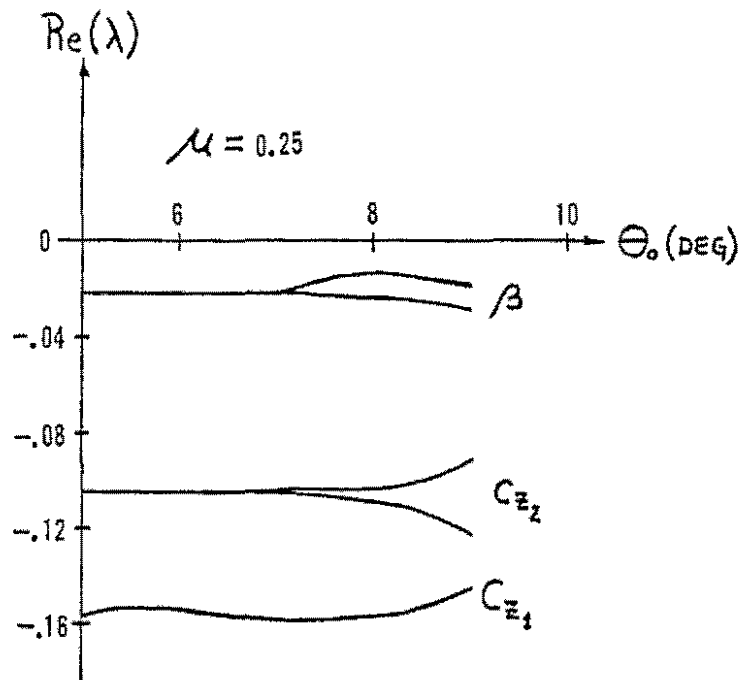


FIGURE 12
DAMPING VERSUS MEAN ANGLE OF ATTACK
 $k=0.05$, $\gamma=6$, $\rho=1$

Figure 12 is a plot of damping versus angle of attack at an advance ratio of 0.25. Here, the β damping remains at the linear value of -0.022 up to an angle of attack of 7° . For angles of attack greater than 7° the root splits into two real parts as indicated in the plot. One root has significantly decreased damping due to the stall effects (-0.014 at 8°). The C_{z_2} damping curve splits after an angle of attack of 6° .

11. SUMMARY AND CONCLUSIONS

The dynamic response of a rotor blade element has been calculated using an analytic stall model to account for non-linearities in lift at high angles of attack. This stall model was developed in Reference 1. In this present research, the model is programmed, verified, and then simplified for use in rotor dynamic analysis. Blade element theory is used to investigate the forced and transient characteristics of the stall model when combined with the flapping dynamics of a rotor blade. The conclusions of these analyses are:

1) The analytic stall model accurately predicts the dynamic stall of oscillating airfoils and has excellent correlation with measured wind tunnel data. (Although some modifications are necessary, Figure 8a for example.)

2) The stall model is simple and can be easily incorporated into a rotor dynamic analysis through the addition of 3 state variables at each blade section. The resulting system may be solved by conventional numerical integration techniques for the forced response; and, after linearization, it may be solved by Floquet theory for the transient response.

3) The perturbation eigenvalue analysis (constant-coefficient or Floquet) gives a physically meaningful indication of the true, non-linear rotor response.

4) Results of an analysis that uses the stall model are more representative of actual blade dynamic response than are those found by classical linearized theory.

Further investigations and refinements of the stall model are necessary to produce a more continuous response throughout the true operating range of blade angle of attack and advance ratio.

12. ACKNOWLEDGEMENTS

The author would like to extend his sincerest gratitude to Dr. David Peters for his guidance and moral support during this research.

This work was sponsored by the United States Army Research Office, Grant No. DAAG-29-80-C-0092. The view, opinions, and/or findings contained in this report are those of the author and should not be construed as an official Department of the Army position, policy, or decision, unless as designated by other documentation.

13. REFERENCES

- 1) Tran, C.T. and Petot, D., "Semi-Empirical Model for the Dynamic Stall of Airfoils in View of the Application to the Calculation of Responses of a Helicopter Blade in Forward Flight," Sixth European Rotorcraft and Powered Lift Forum, Bristol, England, September 1980.
2. Carta, F.O. and Carlson, R.G., "Determination of Airfoil and Rotor Blade Dynamic Stall Response," Journal of the American Helicopter Society, Vol. 18, No. 2, April 1973, pp. 31-39.
- 3) McCroskey, W.J., "Unsteady Airfoils," Annual Review of Fluid Mechanics, Vol. 14, 1982, pp. 285-311.
- 4) McCroskey, W.J., "The Phenomenon of Dynamic Stall," NASA Technical Memorandum 81264, March 1981.
- 5) Bielawa, R.L., "Synthesized Unsteady Airfoil Data with Applications to Stall Flutter Calculations," Proceedings of the 31st Annual National Forum of the American Helicopter Society, Washington, D.C., May 1975.
- 6) Gangwani, S., "Prediction of Dynamic Stall and Unsteady Airloads for Rotor Blades," Proceedings of the 37th Annual National Forum of the American Helicopter Society, New Orleans, May 1981, pp. 1-17.
- 7) Peters, D.A. and Hohensmer, K.H., "Application of the Floquet Transition Matrix to Problems of Lifting Rotor Stability," Journal of the American Helicopter Society, Vol. 16, No. 2, April 1971, pp. 25-33.
- 8) Rogers, Jon P., Application of an Analytic Stall Model to Dynamic Analysis of Rotor Blades, Master of Science Thesis, Washington University, May 1982.